Effect of wave-function localization on the time delay in photoemission from surfaces

C.-H. Zhang and U. Thumm
Department of Physics, Kansas State University, Manhattan, Kansas 66506, USA
(Received 24 October 2011; published 14 December 2011)

We investigate streaking time delays in the photoemission from a solid model surface as a function of the degree of localization of the initial-state wave functions. We consider a one-dimensional slab with lattice constant a_{latt} of attractive Gaussian-shaped core potentials of width σ. The parameter σ/a_{latt} thus controls the overlap between adjacent core potentials and localization of the electronic eigenfunctions on the lattice points. Small values of $\sigma/a_{\mathrm{latt}} \ll 1$ yield lattice eigenfunctions that consist of localized atomic wave functions modulated by a "Bloch-envelope" function, while the eigenfunctions become delocalized for larger values of $\sigma/a_{\mathrm{latt}} \gtrsim 0.4$. By numerically solving the time-dependent Schrödinger equation, we calculate photoemission spectra from which we deduce a characteristic *bimodal* shape of the band-averaged photoemission time delay: as the slab eigenfunctions become increasingly delocalized, the time delay quickly decreases near $\sigma/a_{\mathrm{latt}} = 0.3$ from relatively large values below $\sigma/a_{\mathrm{latt}} \sim 0.2$ to much smaller delays above $\sigma/a_{\mathrm{latt}} \sim 0.4$. This change in wave-function localization facilitates the interpretation of a recently measured apparent relative time delay between the photoemission from core and conduction-band levels of a tungsten surface.

DOI: 10.1103/PhysRevA.84.065403 PACS number(s): 32.80.Rm, 42.65.Re, 79.60.−i

I. INTRODUCTION

Streaked photoemission spectroscopy provides a powerful tool to resolve ultra-fast electronic processes during the interaction of extended ultraviolet (XUV) and infrared (IR) pulses of electromagnetic radiation with matter at the time scale [≈1 atomic unit $= 2.4 \times 10^{-17}$ s $= 24$ attoseconds (as)] of the valence-electron motion in isolated atoms and solids. Applying streaking metrology to neon atoms, Schultze *et al.* [1] recently measured a *relative* photoemission (PE) streaking delay of $\delta\tau_{2p-2s} = 21 \pm 5$ as between the emission of electrons from $2p$ and $2s$ orbitals, indicating an apparent earlier release from the $2s$ orbital. Similarly, for PE from a tungsten surface, a relative streaking delay of $\delta\tau_{\mathrm{CB}-4f} = 110 \pm 70$ as has been measured [2] between electrons emitted from localized $4f$ core and delocalized conduction band (CB) levels, where the release from the $4f$ orbital appears to precede emission from CB levels.

The interpretation of these sub-femtosecond temporal shifts in streaked PE spectra is a matter of current debate. For atomic targets, this debate revolves around the importance of contributions to the PE time delay due to the Coulomb interaction of the photoelectron with the residual ion [3,4], the IR-laser field [3–6], and many-electron effects [1,5]. The detailed interpretation of the PE time delay for solid targets is further complicated by the complex electronic band structure [2], elastic and inelastic scattering of the released photoelectron in the solid [7–9], the excitation of surface and bulk plasmon modes [10], and the dependence on the skin depths of the streaking IR-laser field [8,9]. For example, the relative delay $\delta\tau_{\mathrm{CB}-4f} = 110$ as for PE from the W(110) surface can be reproduced within the strong-field approximation [3] and interpreted as an interference effect in the emission of core electrons from different lattice sites [9]. In an alternative explanation, the same relative delay was related to the difference $\delta\tau_{\mathrm{CB}-4f} = \bar{t}_{\mathrm{CB}} - \bar{t}_{4f}$ between the arrival times of CB and $4f$ core photoelectrons at the surface [2,8], where $\bar{t}_{4f}$ and $\bar{t}_{\mathrm{CB}}$ are the average travel times in the solid of photoelectrons that are released from the $4f$ core-level (CL) and CB states, respectively. A classical simulation including (in)elastic collisions with tungsten cores during the propagation of photoelectrons inside the solid led to a relative delay of $\delta\tau_{\mathrm{CB}-4f} = 33$ as [7], which underestimates the experimental result of Ref. [2].

Defining *absolute* PE time delays based on the temporal shift (or phase shift) between the streaking IR-laser field and streaking trace in the PE emission spectrum, our recent numerical results [11] show that for a vanishing IR-skin depth the absolute delays τ_{CL} and τ_{CB} for PE from localized CL and CB states behave very differently as functions of the photoelectron kinetic energy E_{kin}. $\tau_{\mathrm{CL}}(E_{\mathrm{kin}})$ is given by the average "travel time" inside the solid $\bar{t} = \lambda/\sqrt{2E_{\mathrm{kin}}}$ for photoelectrons that are released at an average depth equal to the electron mean-free-path λ. In contrast, the streaking delay $\tau_{\mathrm{CB}}(E_{\mathrm{kin}})$ strongly deviates from $\bar{t}$ and is nonmonotonic in E_{kin}. The different accumulation of (absolute) time delays for the PE from localized and delocalized levels, in addition to the above-mentioned propagation and collective-excitation effects, makes the interpretation of relative streaking time delays for PE from different levels of solid targets more complex than for gaseous atomic targets [1,11].

In this work, we show that the different behavior of PE time delays in streaked PE experiments from metal surfaces is largely due to the localized vs delocalized nature of initial-state wave functions. To quantitatively examine the dependence of relative PE delays on the wave-function localization, we construct a model electronic lattice potential that consists of identical attractive core potentials on each lattice site. We represent these core potentials as Gaussian functions with an adjustable width σ that determines the overlap of core potentials on neighboring lattice sites. Changing σ will thus allow us to control the degree to which electronic eigenfunctions of the lattice potential are localized near lattice points. This enables us to assess the influence of wave-function localization on the streaked PE spectra by calculating band-averaged time delays for streaked PE as a function of σ. We use atomic units (a.u.) throughout this work unless indicated otherwise.

II. MODEL

We model the one-dimensional solid as a row of N equidistant atoms and represent each atomic core by an effective attractive Gaussian potential to form the lattice potential [11]

$$V(z) = V_0 - \frac{A_0}{\sqrt{2\pi}\sigma}\sum_{i=1}^{N} e^{-[z+(i+1/2)a_{\rm latt}]^2/(2\sigma^2)}, \qquad (1)$$

where $a_{\rm latt}$ is the lattice constant and σ controls the overlap of the two adjacent core potentials.

By diagonalizing the time-independent Schrödinger equation

$$\varepsilon_n\psi_n(z) = \left[-\frac{1}{2}\frac{d^2}{dz^2} + V(z)\right]\psi_n(z), \qquad (2)$$

for $N = 47$, $V_0 = -0.5$, A_0=2, $a_{\rm latt} = 6$, and $\sigma = 0.1a_{\rm latt}$, we obtain a spectrum of substrate states that includes a narrow band of N localized wave functions with energies $\epsilon_n \approx -32$ eV [11]. As we change σ, the wave functions change from being localized at the lattice sites for $\sigma = 0.1a_{\rm latt}$ to fully delocalized for $\sigma = 0.5a_{\rm latt}$ (Fig. 1). While changing σ, we adjust A_0 so that the average potential-well depth $V_0 - A_0/(\sqrt{2\pi}\sigma)$ and the band-averaged binding energy $\varepsilon = \sum_{n=1}^{N}\varepsilon_n P_n/\sum_n P_n$ vary by less than 10%, where P_n is the PE probability from level n.

We solve the time-dependent Schrödinger equation (TDSE) following the numerical-grid-propagation method of Ref. [3] to calculate streaked PE spectra and streaking time delays. First, we propagate each wave function $\psi_n(z)$ in the streaking IR-laser electric field by numerically solving

$$i\frac{\partial}{\partial t}\psi_n(z,t) = \left\{\frac{1}{2}[p + A_L(z,t-\Delta t)]^2 + V(z)\right\}\psi_n(z,t). \qquad (3)$$

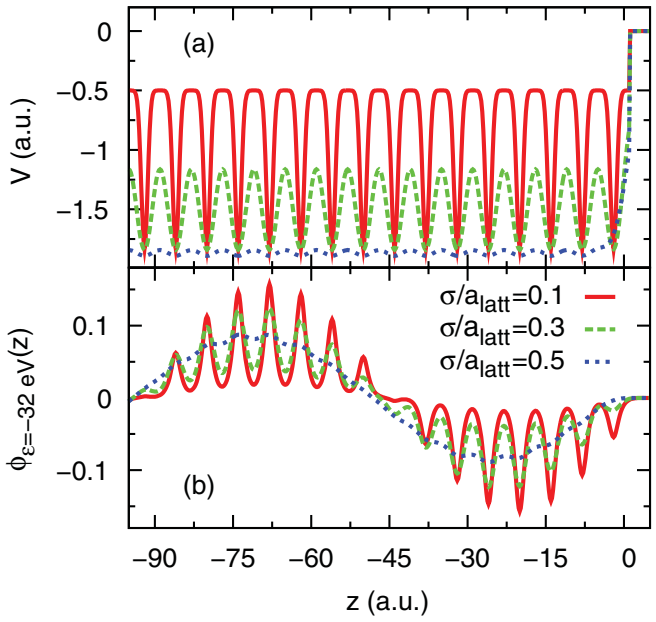

FIG. 1. (Color online) (a) Lattice potential and (b) wave function as a function of the core-potential-width parameter σ for a binding energy of 32 eV. The wave function changes from completely localized at $\sigma = 0.1a_{\rm latt}$ to fully delocalized at $\sigma = 0.5a_{\rm latt}$.

$p = id/dz$ is the momentum operator, and Δt is the delay between the centers of the XUV and IR pulses, using the convention that $\Delta t > 0$ corresponds to the XUV pulse preceding the IR pulse. We model the vector potential of the IR-laser pulse as

$$A_L(t) = A_0\sin^2(\pi t/T_L)\cos[\omega_L(t - T_L/2)] \qquad (4)$$

for $0 \leqslant t \leqslant T_L$ and set A_L to 0 otherwise. We choose a central photon energy of $\hbar\omega_L = 1.57$ eV (corresponding to a wavelength of $\lambda_L = 800$ nm), the peak intensity $I_L = A_0^2\omega_L^2/2 = 5\times10^{11}$W/cm^2, and a pulse length of $T_L = 8$ fs. We further assume an exponential damping of the IR-laser field inside the solid,

$$A_L(z,t) = A_L(t)[e^{z/\delta_L}\Theta(-z) + \Theta(z)], \qquad (5)$$

characterized by the IR-skin depth δ_L.

Next, we calculate the photoelectron wave packet emitted from the nth laser-dressed wave function $\psi_n(z,t)$ by numerically solving the inhomogeneous TDSE,

$$i\frac{\partial}{\partial t}\delta\psi_n(z,t) = \left\{\frac{[p + A_L(z,t-\Delta t)]^2}{2} + V(z)\right\}\delta\psi_n(z,t) + zE_X(t)\psi_n(z,t). \qquad (6)$$

We assume sufficiently low XUV peak intensities, so that the photoelectron release by the XUV pulse can be treated in first-order perturbation theory, and represent the coupling of the electric field E_X of the XUV pulse to the electron in the dipole-length form. We model the XUV pulse,

$$E_X(t) \sim e^{-2\ln 2(t/T_X)^2}\sin(\omega_X t), \qquad (7)$$

with a Gaussian envelope, the pulse duration $T_X = 300$ as, and a variable central frequency ω_X.

Assuming free-electron dispersion ($\varepsilon_k = k^2/2$), the XUV-IR delay-dependent center-of-energy (COE) for PE from a given initial state ψ_n is [9,11]

$$E_{{\rm COE},n}(\Delta t) = \frac{1}{2P_n(\Delta t)}\int dk\,|k\,\delta\phi_n(k,\infty;\Delta t)|^2\,, \qquad (8)$$

with the probability for PE from the initial state ψ_n

$$P_n(\Delta t) = \int dk\,|\delta\phi_n(k,\infty;\Delta t)|^2\,. \qquad (9)$$

$\delta\phi_n(k,\infty;\Delta t)$ is the Fourier transform of $\delta\psi_n(z,T;\Delta t)$, and the time T is chosen large enough for $P_n(\Delta t)$ to have converged. For the numerical results shown in this report we found converged results for $T = 1.5T_L$.

The band-averaged COE follows as

$$E_{\rm COE}(\Delta t) = \frac{1}{\sum_{n=1}^{N}P_n(\Delta t)}\sum_{n=1}^{N}P_n(\Delta t)E_{{\rm COE},n}(\Delta t). \qquad (10)$$

After calculating $E_{\rm COE}(\Delta t)$ for a range of XUV-IR delays, $-T_L/2 \leqslant \Delta t \leqslant T_L/2$, we obtain the band-averaged streaking delay τ_S relative to A_L by fitting the parameters a, b, and τ_S in the expression [3,9]

$$E_{\rm COE}(\Delta t) = a + bA_L(\Delta t - \tau_S). \qquad (11)$$

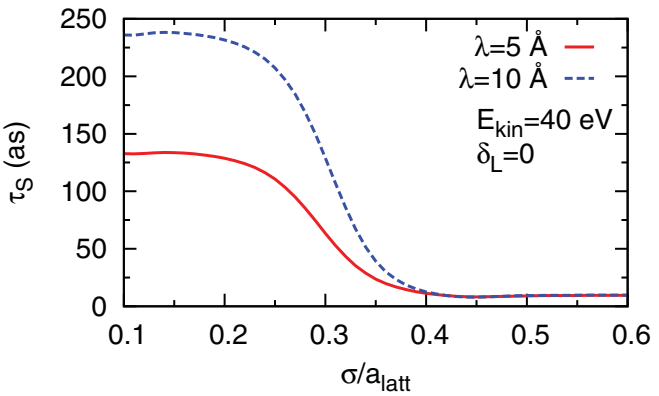

FIG. 2. (Color online) Band-averaged streaking delay as a function of the wave-function-localization parameter $\sigma/a_{\rm latt}$ for two photoelectron mean-free paths λ and the IR-skin depth $\delta_L = 0$. The average photoelectron kinetic energy is $E_{\rm kin} = 40$ eV.

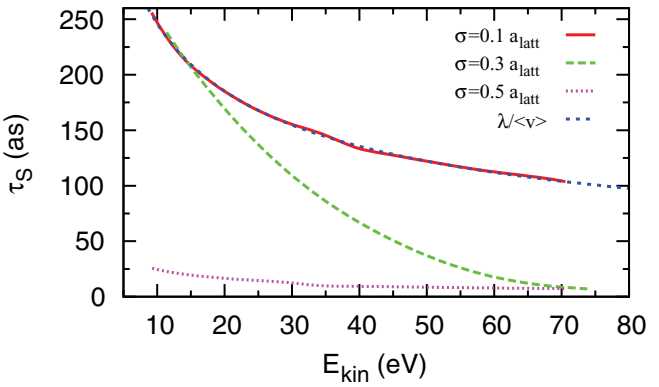

FIG. 3. (Color online) Band-averaged streaking delay as a function of the photoelectron kinetic energy for different wave-function-localization parameters $\sigma/a_{\rm latt}$, $\lambda = 5$ Å, and $\delta_L = 0$.

III. NUMERICAL RESULTS

We calculate band-averaged PE delays τ_S [see Eqs. (10) and (11)] as a function of the overlap parameter σ for the lattice potential $V(z)$. We set the IR-skin depth $\delta_L = 0$ in all calculations below, since for this case only the streaking time delay has a simple interpretation as the time the photoelectron propagates inside the solid before getting exposed to the streaking IR-laser field at the surface [2,8,11]. However, as pointed out in the Introduction, τ_S is proportional to $1/\sqrt{E_{\rm kin}}$ only for emission from localized initial states, while depending in a more complicated way on $E_{\rm kin}$ for PE from delocalized levels [11].

Figure 2 shows the band-averaged streaking delay as a function of the wave-function localization parameter $\sigma/a_{\rm latt}$ for two values of λ and $E_{\rm kin} = 40$ eV. The streaking time delay τ_S decreases very slowly for $\sigma/a_{\rm latt} \lesssim 0.2$, i.e., for PE from localized initial states. It then quickly decreases in a transition region near $\sigma \sim 0.3a_{\rm latt}$, where the wave-function character changes from localized to delocalized, and eventually stabilizes at a small delay time for $\sigma \gtrsim 0.4a_{\rm latt}$, where the wave function becomes fully delocalized. The numerical results in this figure confirm that the streaking delay becomes insensitive to the mean-free path for PE from (mostly) delocalized states with $\sigma/a_{\rm latt} > 0.4$, for which $\tau_S(\lambda = 5\text{Å}) = \tau_S(\lambda = 10\text{Å})$ within the width of the two curves in this figure.

The dependence of the band-averaged streaking delay τ_S on the average kinetic energy of the photoelectron $E_{\rm kin}$ for three values of $\sigma/a_{\rm latt}$ is shown in Fig. 3. For PE from a localized initial state with $\sigma/a_{\rm latt} = 0.1$, our numerical results confirm the interpretation given above: τ_S can be understood as the average time $\lambda/\sqrt{2E_{\rm kin}}$ needed for released photoelectrons to travel an average distance λ inside the solid with velocity $\sqrt{2E_{\rm kin}}$. Moreover, for the set of parameters used in these calculations ($\lambda = 5$ and 10 Å, $\delta_L = 0$) and within the resolution of the figure, τ_S (solid curve) and $\lambda/\sqrt{2E_{\rm kin}}$ (short-dashed curve) are identical. However, this interpretation starts to break down if we increase $\sigma/a_{\rm latt}$, thereby describing PE from increasingly delocalized initial states, and quickly becomes invalid for larger values of $\sigma/a_{\rm latt}$. This behavior is clearly seen in the numerical data: for intermediate delocalization ($\sigma/a_{\rm latt} = 0.3$), $\tau_S(E_{\rm kin})$ (green dashed curve) rapidly starts to deviate from the estimated average travel time $\lambda/\sqrt{2E_{\rm kin}}$ (blue dotted curve) as $E_{\rm kin}$ is increased above ≈ 15 eV. Furthermore, for PE from a fully delocalized initial state ($\sigma/a_{\rm latt} = 0.5$, pink dotted line), $\tau_S(E_{\rm kin})$ decreases very slowly as a function of $E_{\rm kin}$ and strongly deviates from $\lambda/\sqrt{2E_{\rm kin}}$ over the entire range of kinetic energies shown in this figure.

The kinetic energies in the streaking experiment of Cavalieri *et al.* [2] are ~55 and ~81 eV for XUV PE from the $4f$ CLs and the CB, respectively. Assuming that the streaking IR-laser field is fully screened inside the metal, and noting the bimodal behavior of the streaking time delay as a function of the localization parameter (cf. Fig. 2), we may assign parameter values $\sigma = 0.1a_{\rm latt}$ to the localized $4f$ levels of tungsten and any value $\sigma \gtrsim 0.3a_{\rm latt}$ to the delocalized CB levels. With this assignment, a relative streaking time delay $\delta\tau_{{\rm CB}-4f} = 120$ as can be deduced from Fig. 3. Interestingly, this relative time delay coincides with the value measured by Cavalieri *et al.* of 110 ± 70 as, despite the fact that, apart from their localization character, the initial states of our simulation have little in common with core and CB levels of the tungsten target used in the experiment. Since the band-averaged streaking time delay ceases to be sensitive to the initial-state wave-function localization for $\sigma \gtrsim 0.3a_{\rm latt}$ and $E_{\rm kin} \gtrsim 60$ eV (cf. Fig. 3), future experiments would have to use smaller XUV-photon energies (resulting in $E_{\rm kin}$ clearly below 60 eV) in order to probe the localization properties of the initial-state wave functions.

IV. CONCLUSION

We investigated streaking delays in the PE from model solid surfaces as a function of the degree of localization of the initial-state wave functions. Our numerical results show a characteristic bimodal behavior of the streaking delay, with large (small) delays for PE from localized (delocalized) states, and confirm different interpretations for the accumulation (or lack thereof) of streaking time delays during the PE from localized (delocalized) initial states of a solid target.

ACKNOWLEDGMENTS

This work was supported by the NSF and the Division of Chemical Sciences, Office of Basic Energy Sciences, Office of Energy Research, US DOE. The computations for this project were performed on the Beocat cluster at Kansas State University.

[1] M. Schultze *et al.*, Science **328**, 1658 (2010).
[2] A. L. Cavalieri *et al.*, Nature **449**, 1029 (2007).
[3] C.-H. Zhang and U. Thumm, Phys. Rev. A **82**, 043405 (2010).
[4] S. Nagele, R. Pazourek, J. Feist, K. Doblhoff-Dier, C. Lemell, K. Tőkési, and J. Burgdörfer, J. Phys. B **44**, 081001 (2011).
[5] A. S. Kheifets and I. A. Ivanov, Phys. Rev. Lett. **105**, 233002 (2010).
[6] I. A. Ivanov, Phys. Rev. A **83**, 023421 (2011).
[7] C. Lemell, B. Solleder, K. Tökési, and J. Burgdörfer, Phys. Rev. A **79**, 062901 (2009).
[8] A. K. Kazansky and P. M. Echenique, Phys. Rev. Lett. **102**, 177401 (2009).
[9] C.-H. Zhang and U. Thumm, Phys. Rev. Lett. **102**, 123601 (2009); **103**, 239902(E) (2009).
[10] C.-H. Zhang and U. Thumm, Phys. Rev. A **84**, 063403 (2011).
[11] C.-H. Zhang and U. Thumm, Phys. Rev. A **84**, 033401 (2011).